C432/151

Bearing parameter identification using power spectral density methods

C ROUVAS, BS, MS, MASME
Department of Mechanical Engineering, Texas A&M University, College Station, Texas, United States of America
B T MURPHY, PhD, MASME
Rocketdyne, Canoga Park, California, United States of America
R K HALE, BSIE
Department of Mechanical Engineering, Texas A&M University, College Station, Texas, United States of America

Abstract

The most direct means of measuring rotordynamic coefficients for fluid film bearings is to measure the bearing force and deflection during a dynamic condition, and then to use some type of data reduction procedure to compute the required stiffness, damping and inertia values. Numerous works have been recently published on this topic. One goal of the data reduction process is to minimize, if not eliminate, the effects of signal noise inevitably superimposed on the "true data". There are many different aspects of the data reduction problem which must be properly addressed in order to produce the most accurate result possible (i.e. minimize the overall experimental uncertainty). The purpose of this paper is to show how certain advanced signal processing techniques developed in the field of modal analysis (among others) can be used to suppress signal noise. It is shown by example with actual data from a hydrostatic bearing test apparatus how proper application of these techniques can reduce not only random errors, but also all important bias errors.

Nomenclature

a_x, a_y : bearing acceleration in x, y direction
f : frequency
f_x, f_y : impact force in x, y direction
j : imaginary number ($\sqrt{-1}$)
t : time
n_d : number of averages
$u(t)$: input to single input, single output system
$v(t)$: output of single input, single output system
A_x, A_y : Fourier transform of a_x, a_y
$C_{xx}, \cdots$: damping coefficients
F_x, F_y : impact force in x, y direction
G_{ii} : auto spectral density
G_{ij} : cross spectral density
H_{uv} : FRF of single input, single output system
$H_{xx}, \cdots$: frequency response functions
$K_{xx}, \cdots$: stiffness coefficients
M_b : bearing mass
$M_{xx}, \cdots$: mass coefficients
$N(f)$: noise
R_x, R_y : reference signals
T : total sampling time.
$U(f)$: Fourier transform of $u(t)$
$V(f)$: Fourier transform of $v(t)$
X, Y : Fourier transform of δx, δy
δx, $\delta \dot{x}$, $\delta \ddot{x}$: displacement, velocity, acceleration of bearing with respect to shaft, in the x direction
δy, $\delta \dot{y}$, $\delta \ddot{y}$: displacement, velocity, acceleration of bearing with respect to shaft, in the y direction
ϕ : phase angle
ω : frequency ($2\pi f$)
Δt : time shift
$\Delta\phi$: phase angle difference
$(\ )^x$: response ( ) due to impact in the x direction
$(\ )^y$: response ( ) due to impact in the y direction
$(\ )^*$: transpose of the complex ( )

Introduction

With the advent of high performance turbomachinery accurate estimation of bearing parameters has become increasingly important. Many researchers have undertaken this task, resulting in a wealth of parameter identification methods for rotordynamic stiffness, damping, and sometimes inertia coefficients (from hereon denoted KCM). These methods can be broadly classified as either time domain or frequency domain methods, in accordance with whether the actual calculation of the KCM values is carried out in the time or frequency domain. Murphy et al. [1], discussed several frequency domain methods in detail, and reviewed the major published efforts in this area. They also cited some of the key groups developing time domain methods. It is the opinion of these authors that frequency domain methods are better suited for measurement of KCM values primarily because the KCM values are themselves frequency based parameters. For example, the stiffness (K) values model forces which are independent of frequency. The damping (C) values model forces which are proportional to frequency, and the inertia (M) values model forces proportional to frequency squared. In light of this, the focus of the present paper is on suppression of signal noise for frequency domain methods. This will be accomplished through the use of cross and auto spectral density func-

tions [2]. The use of these frequency domain functions has already become an important part of modal testing [3].

As will be seen, these functions provide a great deal of control over the data averaging process. Their application will be demonstrated in the measurement of KCM values for a hydrostatic bearing. When testing a hydrostatic bearing the signal to noise ratio suffers due to the highly turbulent flow passing through the tester, and also rotational disturbances (unbalance, slave bearings, couplings, gears, etc.). The methods developed here are for tests conducted with instrumented impact hammers, but are readily adaptable to any other test scheme.

In this paper the term power spectral density (PSD) will be used to refer to both auto and cross spectral densities. For transient signals energy spectral densities are the appropriate physical quantities, but since they differ only by a factor of T it makes no difference which ones are used for the determination of frequency response functions (FRF). Halvorsen [4] gives a simple introduction to power spectral density methods. Cawley [5] also addresses some of the aspects of power spectral density computations. He deals with single input, single output systems, subjected to transient excitation, with a focus on the accuracy of the determination of the FRF maxima and minima.

Nordmann [6] used impact excitation to identify bearing characteristics. Mobilities were determined by direct averaging of the input and output signals, and coefficients were extracted by non-linear least squares curve fits on the mobilities. Yasuda et al. [7] used power spectral densities to extract the coefficients of a bearing subjected to random excitation. Overall, the capabilities of power spectral density methods have not yet been fully explored in the field of rotordynamics. It is the purpose of this paper to address some of these issues and provide guidelines for the effective application of PSDs in rotordynamic coefficient calculations.

Experimental Setup

Testing was performed at the Texas A&M University Hydrostatic Bearing Test Facility. A complete description of the test rig and its capabilities is given by Kurtin et al.[8]. Here only an outline of the dynamic test setup will be given. The test section is shown in Fig. 1. The high speed shaft is supported by two hydrostatic bearings, and the test bearing floats freely at the midsection. The shaft is rotated by an electric motor, through a speed increasing gearbox, at speeds up to 25,000 rpm. The bearings are lubricated with heated water (54.4 C, 130F), at 7.0 MPa (1000 psi). The test bearing geometry is shown in Fig. 2, with specifications and test operating conditions given in Table 1.

Two orthogonally mounted impact hammers are used to excite the floating bearing housing. Rigid mounting allows repeatable forces to be applied to the bearing. The impact hammer tips used were medium hardness vinyl tips, a compromise between high wear rates of softer tips, and low impact energies at the frequencies of interest for harder tips. The hammers have a maximum rating of 4.45 KN (1000 lb) peak applied load. Impact excitation is simple to apply, and provides broad band excitation, but is prone to poor signal to noise ratios (S/N) in part because of high crest factor (peak value/rms value). The poor S/N ratio can be counteracted by increasing the amplitude of the impact force, or by repeating the experiment and using averaging. Care should be taken when increasing the impact force not to force the bearing into nonlinear operation.

The instruments used for the dynamic measurements are the impact hammer load cells, accelerometers and eddy current proximitors for each of the x and y directions. The accelerometers are mounted at the bearing midplane opposite from the impact hammers. Two motion probes are mounted in each plane, at the ends of the bearing housing. In the data reduction process the bearing deflection at midplane is obtained by averaging the measured deflections at the ends of the bearing. Transducer signals are sampled simultaneously by a high speed data acquisition unit. The readings are downloaded to a PC where they are stored for analysis. All signals are passed through matched anti-aliasing filters, with a cutoff frequency of 500 Hz, before sampling. For each hammer strike readings are taken at 10240 samples/sec/channel over a 0.1 second period, yielding a 1024 sample size, and a 10 Hz frequency resolution. Data acquisition is triggered by the rising side of the impact force signal, with 100 pre-trigger samples recorded.

Repeatability in the impact data was achieved by data capture to the data acquisition system to initiate at an impact force level of 700 N, which corresponded to the region of abrupt force change. The sampling rate was set to provide an accurate definition of the impact pulse.

Modeling

1. Basic concepts

Some of the concepts involved in the determination of frequency response functions can be illustrated by a single input-single output system, with input $u(t)$ and output $v(t)$. The frequency response function (FRF) of the system, in the frequency domain is given by

$$H_{uv}(f) = V(f)/U(f). \tag{1}$$

If the output V is contaminated by noise N then the FRF will be overestimated by N/U. The bias can be minimized by averaging, hence

$$H_{uv}(f) = \frac{\sum_{i=1}^{n_d} V_i(f)/n_d}{\sum_{i=1}^{n_d} U_i(f)/n_d}. \tag{2}$$

For n_d averages, and Gaussian noise, the signal to noise ratio (S/N) improvement will be $\sqrt{n_d}$. Since the Fourier transform is a linear transformation, the same result for H_{uv} can be obtained by using Eq. 1 with time domain averages of the signals, $u(t)$ and $v(t)$. This formulation assumes that the input U is (a) noise free and (b) repeatable. Noise in U will cause the FRF to be underestimated.

The term non-repeatability is taken here to mean non-repeatable data capture initialization, so that the impact appears in different locations of the sampling window. A time delay between two identical impacts will translate only to a phase change in the frequency domain. To illustrate the effect of such phase differences consider two

equal amplitude phasors, $u_1 = U\cos(2\pi ft + \phi_1)$ and $u_2 = U\cos(2\pi ft + \phi_2)$. Their average is given by

$$\bar{u} = \frac{u_1 + u_2}{2} = \left(U\cos\frac{\Delta\phi}{2}\right)\cos(2\pi ft + \frac{\phi_1 + \phi_2}{2}), \quad (3)$$

where $\Delta\phi$ is the phase difference between u_1 and u_2. The amplitude of the averaged signal decreases by $\cos(\Delta\phi/2)$, and its phase is shifted to $(\phi_1 + \phi_2)/2$. In the worst possible case $\Delta\phi$ is 180 deg, and all information about that frequency is lost, while at the other extreme $\Delta\phi$ is zero (i.e. the signal is exactly repeatable), and no information is lost.

For a linear system the amplitudes and phases of the input and output will be scaled and shifted by the same amount, therefore the estimate of the FRF should not be adversely affected by averaging. In the presence of noise though, the scaling effect of the averaging process will not allow the maximum possible increase in the S/N ratio to be attained. Also, if the phase differences are large, the computer accuracy could become a problem.

If a time domain signal is shifted by Δt, then each of its frequency components will experience a phase change of $\Delta\phi = 2\pi f\Delta t$. For the same time shift Δt, higher frequencies will have a higher phase shift, which will make them more susceptible to the errors discussed above.

These problems of time domain averaging can be circumvented by the use of power spectral densities. The cross spectral density Guv is defined as

$$G_{uv} = \lim_{T\to\infty}\frac{2}{T}E[U^*(f)V(f)] \quad (4)$$

For a simple introduction to PSD methods see Halvorsen [4]. To obtain an H_{uv} estimate using PSDs, the numerator and denominator of Eq. 1 are multiplied by $U^*(f)$. By taking the expected values of each product, multiplying by $2/T$ and taking the limit as T approaches infinity, the FRF estimate is found to be:

$$H_{uv}(f) = \frac{G_{uv}(f)}{G_{uu}(f)}. \quad (5)$$

For noise-free input, Eq. 5 gives an unbiased estimate of the FRF [2]. For finite record lengths the PSD G_{uv} is estimated by

$$G_{uv}(f) = \frac{2}{n_d N\Delta t}\sum_{i=1}^{n_d} U^*(f)V(f). \quad (6)$$

If the input signal is exactly repeatable (i.e. $U_1(f) = U_2(f) = \cdots = U_{n_d}(f)$) then Eq. 5 is equivalent to the time domain averaging Eq. 2. If not, then the use of PSDs will prevent the loss of information that occurs with direct averaging, because the PSD is a summation of power-like, quantity-squared terms. For testing, this means that averaging with Eq. 4 is insensitive to fluctuations, in both trigger time and peak applied loads.

2. Bearing model

The equations of motion for the floating bearing housing are obtained by applying Newton's 2nd law.

$$\begin{Bmatrix} f_x - M_b a_x \\ f_y - M_b a_y \end{Bmatrix} = \begin{bmatrix} K_{xx} & K_{xy} \\ K_{yx} & K_{yy} \end{bmatrix}\begin{Bmatrix} \delta x \\ \delta y \end{Bmatrix} +$$

$$\begin{bmatrix} C_{xx} & C_{xy} \\ C_{yx} & C_{yy} \end{bmatrix}\begin{Bmatrix} \delta\dot{x} \\ \delta\dot{y} \end{Bmatrix} + \begin{bmatrix} M_{xx} & M_{xy} \\ M_{yx} & M_{yy} \end{bmatrix}\begin{Bmatrix} \delta\ddot{} \\ \delta \end{Bmatrix}$$

The added mass terms M_{ij} are due to the fluid inertia in the bearing and were predicted by San Andres [9] to have a significant effect on hydrostatic bearing operation. The Fourier transform is used to transform these equations to the frequency domain resulting in:

$$\begin{Bmatrix} F_x - M_b A_x \\ F_y - M_b A_y \end{Bmatrix} = \begin{bmatrix} H_{xx} & H_{xy} \\ H_{yx} & H_{yy} \end{bmatrix}\begin{Bmatrix} X \\ Y \end{Bmatrix} \quad (8a)$$

$$H_{ij} = K_{ij} - \omega^2 M_{ij} + j\omega C_{ij} \quad (8b)$$

In Eq. 8b the H_{ij} are complex valued FRFs, and the KCM are expected to be real valued, but the theory does allow for complex valued KCM. In order to completely determine the H_{ij} from Eq. 8a, two "sufficiently different" excitations must be applied separately to the bearing [1]. Here, an x direction impact is used as the first excitation, and a y direction impact as the second. The time domain data acquired for the pair of impacts is transformed to the frequency domain via Fourier Transform. Utilizing the two load cases for each frequency in the test frequency range, the following matrix equation can be written:

$$\begin{bmatrix} F_x - M_b A_x^x & -M_b A_x^y \\ -M_b A_y^x & F_y - M_b A_y^y \end{bmatrix} = \begin{bmatrix} H_{xx} & H_{xy} \\ H_{yx} & H_{yy} \end{bmatrix}\begin{bmatrix} X^x & X^y \\ Y^x & Y^y \end{bmatrix} \quad (9)$$

It is seen that Eqs. 9 can be solved directly for the H's if the displacement matrix in not singular. The real and imaginary components of each H can be plotted versus frequency. Polynomial curve fits of the data directly yield the real and imaginary parts of each K, C and M according to Eq. 8b. It is important to always inspect the H vs. frequency plots to verify that the impedance components are well defined quadratics. Any deviation from a pure quadratic either indicates an error or an unexpected higher order effect.

In the foregoing analysis only a single pair of impacts was required such that there was no data averaging taking place. To reduce random errors in the KCM values, the execution of multiple impacts is carried out so that some type of averaging can be performed. Random errors in the KCM values are reduced by roughly $\sqrt{n_d}$ where n_d is the number of impacts [2]. Different averaging schemes, however, can produce different results. Several such averaging schemes will be considered in the next section.

For time domain averaging, the elements of Eqs. 9 are replaced by their ensemble averages. To formulate the equations of motion in terms of PSDs, first the X and Y impact equations are divided by two arbitrary signals R_x and R_y respectively.

$$\begin{bmatrix} \frac{F_x}{R_x} - M_b\frac{A_x^x}{R_x} & -M_b\frac{A_x^y}{R_y} \\ -M_b\frac{A_y^x}{R_x} & \frac{F_y}{R_y} - M_b\frac{A_y^y}{R_y} \end{bmatrix} =$$

$$\begin{bmatrix} H_{xx} & H_{xy} \\ H_{yx} & H_{yy} \end{bmatrix}\begin{bmatrix} \frac{X^x}{R_x} & \frac{X^y}{R_y} \\ \frac{Y^x}{R_x} & \frac{Y^y}{R_y} \end{bmatrix} \quad (10)$$

The signals R_x, R_y can be chosen to be any of the measured signals, or combination of them, e.g. impact force, motion.

The terms F_x/R_x, A_x^x/R_x, X^x/R_x, $\cdots$ can be considered as frequency response functions of SISO systems, with the FRFs $[H]$ given by a combination of these SISO systems according to Eqs. 10. By applying Eq. 5 to the terms of Eqs. 10, and simplifying common denominators, the equations of motion become

$$\begin{bmatrix} G_{R_xF_x} - M_b G_{R_xA_x^x} & -M_b G_{R_yA_x^y} \\ -M_b G_{R_xA_y^x} & G_{R_yF_y} - M_b G_{R_yA_y^y} \end{bmatrix} = \begin{bmatrix} H_{xx} & H_{xy} \\ H_{yx} & H_{yy} \end{bmatrix} \begin{bmatrix} G_{R_xX^x} & G_{R_yX^y} \\ G_{R_xY^x} & G_{R_yY^y} \end{bmatrix}. \quad (11)$$

Note that Eqs. 11 could also be obtained by multiplying Eqs. 9 by R_x^*, R_y^*, taking expected values, and multiplying the result by $2/T$, with T approaching infinity. The advantage of using Eqs. 10 as an intermediate step is that a formulation in terms of simple SISO systems is provided, thus allowing more insight into the final Eqs. 11.

Results

As mentioned above, R_x and R_y can be chosen to be any of the measured signals, or combination of them. The following cases will be considered :

(i) The impact forces are used as reference signals, $R_x = F_x$, $R_y = F_y$.

(ii) Total forces are used as reference signals, $R_x = F_x - M_b A_x^x$, $R_y = F_y - M_b A_y^y$.

(iii) Motion signals are used as reference, $R_x = X^x$, $R_y = Y^y$.

For the selection of R_x and R_y the guidelines for a SISO system, outlined in the introduction can be used. Plots of typical force, acceleration and motion measurements are given in Fig. 3. The main criterion is that the reference signals be noise free, which is satisfied by the impact force signals.

Plots of frequency response functions for each of cases (i), (ii) and (iii) are shown in Figs. 4, 5 and 6 respectively. All the FRFs demonstrate significant deviations at approximately 330 Hz (20000 rpm), due to the unbalance response of the bearing. This, and its adjacent frequencies are not used in the subsequent curve fits. In all cases the power spectral densities were estimated using 200 test repetitions. The use of impact forces as reference signals (case i) yields the best results, and the use of motion signals as references yields the worst FRF estimates; the scatter in the FRF estimates taken to be a measure of goodness. These results can be explained by the fact that the impact force signals are almost completely noise free, while the motion signals include a considerable amount of noise. In fact, the level of transient response in the motion signals is barely above the noise level. The acceleration signals have only a mild noise content, which causes a very small degradation of the results when the total forces are used as reference signals, compared to the impact-force-reference case.

Repeatability of the impact forces is quantified by the variance of the peak force, and the time at which it occurs. To illustrate the effect of non repeatable excitation forces when time domain averaging is used, the experimental data were given a small random shift of their time base according to values generated by a random number generator. Each data set was shifted such that the peak force occurred within ± 10 time increments from its original location.

The FRFs obtained with time averaging on the original data (Fig. 7) are almost identical to those obtained using the power spectral density formulation, with the impact forces used as the reference signals (Fig. 4). On the other hand, the FRFs obtained from the time shifted data, and time domain averaging (Fig. 8) show considerable variation at higher frequencies, while lower frequencies are not affected by the time shift. This is an expected result, in agreement with the explanation set forth earlier. Use of the power spectral density formulation (Eqs. 11) with the time shifted data gives results identical to those obtained from the original data (cases i, ii and iii above).

The bearing coefficients are obtained from least squares curve fits of the real and imaginary parts of the FRFs. Table 2 shows these coefficients, and their standard deviations.

Conclusion

In this paper it has been shown how a two input, two output system model of a bearing can be reduced to a combination of single input, single output system models. By selecting an appropriate noise free signal as the input to these SISO systems the effects of noise can be minimized. Also the usage of PSDs allows for the impact force to be non-repeatable. If time domain averaging is used with non-repeatable inputs, then some loss of information will occur, but the usage of PSDs alleviates this problem.

The procedures outlined here provide an intuitive approach to the problem and are simple to apply. As such they can be easily modified to apply to other systems, without having to get involved with the mathematical and statistical properties of power spectral densities.

To summarize, power spectral density methods, typically reserved for modal analysis with random excitation have been successfully applied to the bearing parameter identification problem. It was also shown that the method can be used to advantage with deterministic excitation, if the signals are non-repeatable.

References

1 Murphy B. T., Scharrer J. K., Sutton R. F., 1990, "The Rocketdyne Multifunction Tester. Part I: Test Method", Workshop on Rotordynamic Instability Problems in High Performance Turbomachinery, Texas A&M University.

2 Bendat J. S., Piersol A. G., 1986, "Random Data. Analysis and Measurement Techniques", 2nd Edition, Wiley Interscience.

3 Ewins D. J., 1986, "Modal Testing: Theory and Practice", Bruel and Kjaer.

4 Halvorsen W., Brown D., 1977, "Impulse Technique for Structural Frequency Response Testing", Sound and Vibration Magazine, Nov., pp. 8–21.

5 Cawley P., 1985, "The Accuracy of Frequency Response Function Measurements Using FFT Based Analyzers With Transient Excitation", ASME Paper No. 85-DET-44.

6 Nordmann R., Schollhorn K., 1980, "Identification of Stiffness and Damping Coefficients of Journal Bearings by Means of the Impact Method", IMechE Second International Conference, Vibrations in Rotating Machinery, Paper C285/80, pp.231–258.

7 Yasuda C., Kanki H., Ozawa Y., Kawakami T., 1986, "Application of Random Excitation Technique to Dynamic Characteristics Measurement of Bearing", The International Conference on Rotordynamics, Tokyo, pp. 61–67.

8 Kurtin K. A., Childs D. W., San Andres L. A., Hale K., 1991, "Experimental vs. Theoretical Characteristics of a High Speed Hybrid (Combination Hydrostatic and Hydrodynamic) Bearing", STLE/ASME 1991 Tribology Conference, ASME Paper No. 91-Trib-35.

9 San Andres L. A., 1990, "Turbulent Hybrid Bearings with Fluid Inertia Effects", ASME Journal of Tribology, vol. 112.

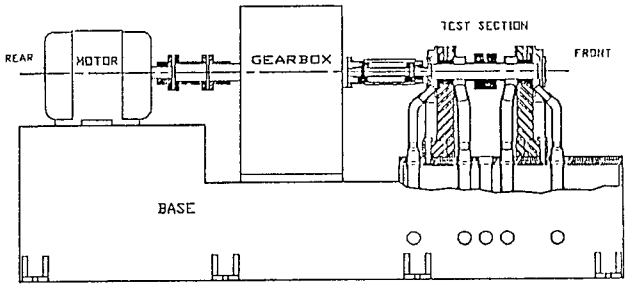

Fig. 1 Test section

Bearing Diameter	: 7.72 cm (3.00 in)
L/D Ratio	: 1.0
Radial Clearance	: 0.076 mm (0.003 in)
Bearing Mass	: 11.34 kg (25 lb)
No. of Recesses	: 5
Operating Speed	: 20000 rpm
Supply Pressure	: 7.0 MPa (1000 psi)
Supply Temperature	: 54 C (130 F)
Eccentricity Ratio	: 0.0

Table 1. Bearing Specifications

	K (MN/m)	C (kN s/m)	M (kg)
XX	124.4(2.8)	234.3(1.8)	6.7(1.3)
XY	185.1(2.4)	24.0(1.6)	-7.7(1.1)
YX	-230.7(1.8)	-14.7(3.4)	7.1(0.8)
YY	118.9(2.2)	211.2(1.6)	0.3(1.0)

Table 2.
Rotordynamic coefficients (standard deviations)

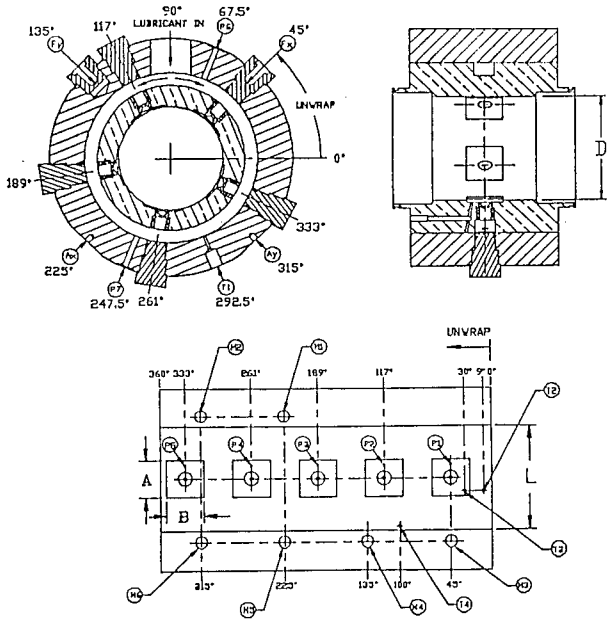

Fig. 2 Test bearing

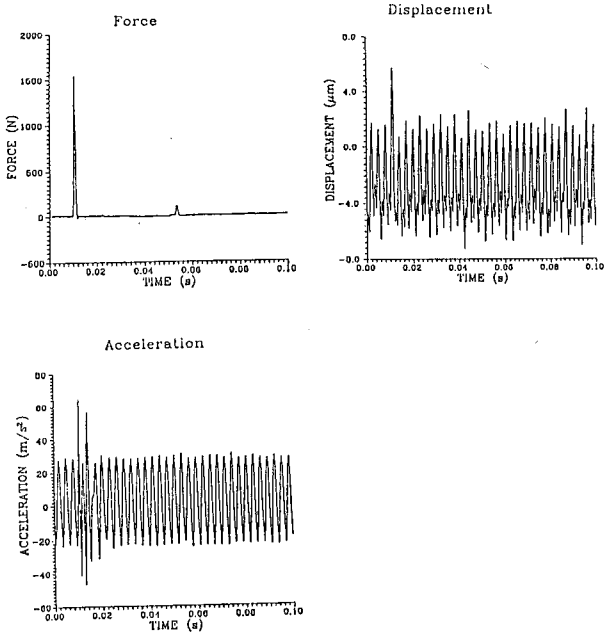

Fig. 3 Time domain histories

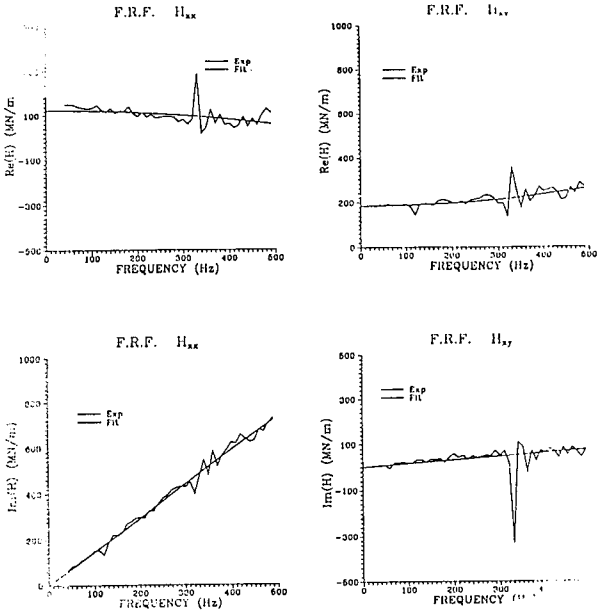

Fig. 4 FRFs, Impact force reference (case i)

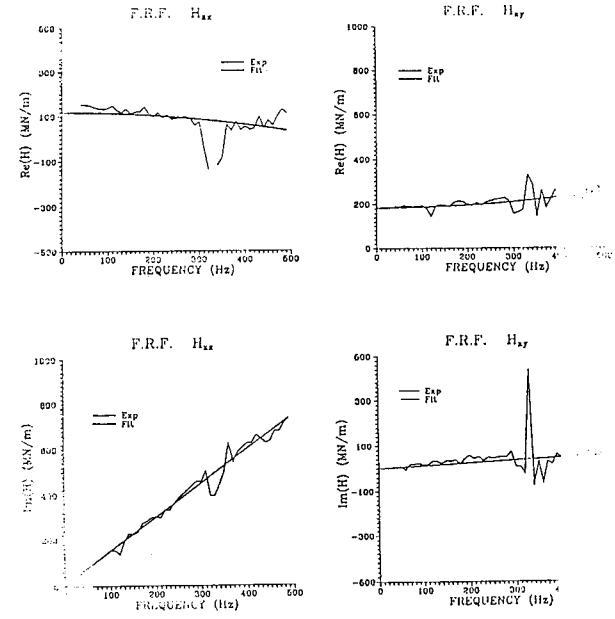

Fig. 5 FRFs, Total force reference (case ii)

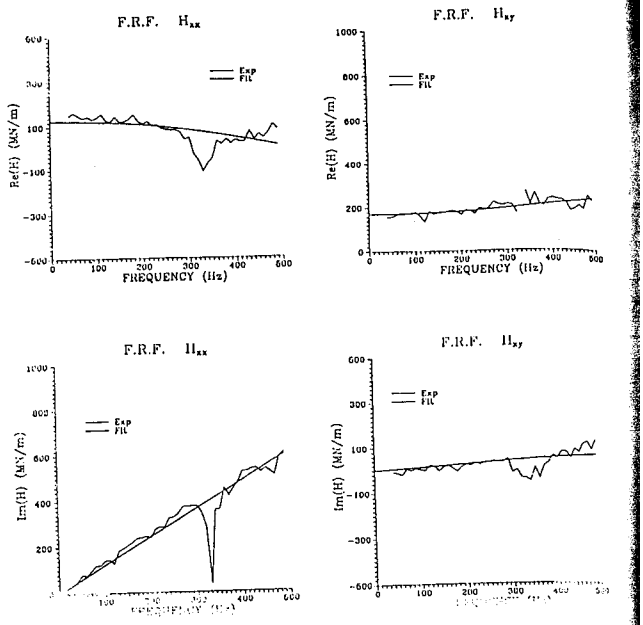

Fig. 6 FRFs, Motion signal reference (case iii)

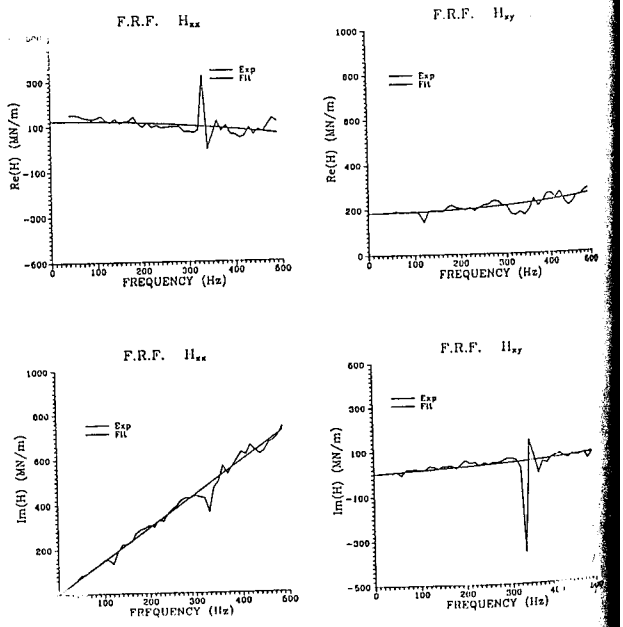

Fig. 7 FRFs, Time domain averaging

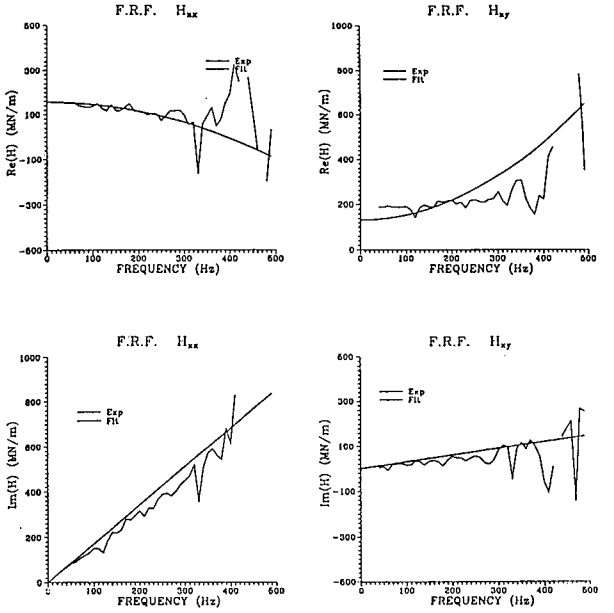

Fig. 8 FRFs, Time domain averaging, non-repeatable data